Electronic Supplementary Material (ESI) for Physical Chemistry Chemical Physics.

Electronic Supplementary Information for: Crucial Role of Electron Transfer from Interfacial Molecules in Negative Potential Shift of Au Electrode Immersed in Ionic Liquid

Taichi Inagaki*†, Norio Takenaka†‡, and Masataka Nagaoka*†‡ §

†*Graduate School of Informatics, Nagoya University, Furo-cho, Chikusa-ku, Nagoya 464-8601, Japan*

‡*Elements Strategy Initiative for Catalysts and Batteries (ESICB), Kyoto University, Nishikyo-ku Kyoto 615-8510, Japan*

§ *Core Research for Evolutional Science and Technology, Japan Science and Technology Agency, Honmachi, Kawaguchi 332-0012, Japan*

E-mail: inagaki@ncube.human.nagoya-u.ac.jp; mnagaoka@i.nagoya-u.ac.jp

Phone: +81 (0)52 789 5623. Fax: +81 (0)52 789 5623

1. Computational Details for Classical Molecular Dynamics Simulations

In order to sample a number of uncorrelated ionic liquid configurations, we performed classical molecular dynamics simulations. The equations of motion were integrated using a standard velocity-Verlet integrator with a time step of 1.0 fs and bonds including a hydrogen atom were held rigid by the SHAKE/RATTLE method[S1]. We employed the particle-particle particle-mesh Ewald scheme [S2] for the electrostatic interaction, where long-range interactions beyond a cutoff of 7.0 Å were computed in the reciprocal space. Short-range electrostatic and van der Waals interactions were treated by a pairwise calculation within the cutoff length of 7.0 Å. During the simulations the Au electrode atoms were fixed at the ideal fcc(111) geometry. In addition, as mentioned in the main text, we used a constant zero-charge model for the electrode atoms. Although this model neglects polarization of the metal electrode surface as a perfect conductor, the polarization was demonstrated not to affect significantly the IL configurations near the surface by constant potential simulations like that proposed by Reed and coworkers[S3].

A force field proposed by Köddermann and coworkers[S4] was used for the TFSA and BMIM molecules. For Au atoms a parameterization via 12-6 Lennard-Jones interactions for face-centered cubic metals by Heinz and coworkers[S5] was used to describe the short-range van der Waals interactions with IL molecules. This force field parameter set is the same as in the work of Ferreira and coworkers[S6].

2. Sampling Procedure for Ionic Liquid Configurations

A number of ionic liquid configurations were sampled by using the classical molecular dynamics simulations with the whole system (Figure 1 in the main text). Ten configurations were picked up every 100 ps step from a 1 ns simulation with temperature of 1000 K. Using each configuration as an initial structure, next cooling simulations with a cooling speed of 100 K/ns were performed until the system temperature reaches 300 K. After that, simulations at 300 K were performed with 10 ns duration, whose final configurations were used as the initial configurations for the first-principles calculations. This process was repeated five times with different initial structures from each other for the 1000 K simulations, resulting in 50 independent configurations. This number of configurations is shown in the main text to be sufficient to calculate the reasonable averaged potential shift.

3. Occupied Molecular Orbital Contributions to Conduction Band

In the main text, from the molecular orbital (MO)-projected densities of states (DOSs) (Figure 7b), we observed the occupied MOs penetrating above the Fermi level. This observation provided the valid evidence for the electron transfer from the cationic BMIM molecule to the Au electrode surface. In addition to the valuable insight we obtained another insight into which MO contributes largely to the electron transfer. Figure S1a displays the ratio of the contributions of each occupied MO in the isolated IL molecules (a BMIM cation and a TFSA anion) to the conduction band at 0.05 eV above the Fermi level. Note that the ratio is relative to the total contribution of all occupied MOs, not to the whole conduction band at the energy. The largest contributions from the TFSA and BMIM molecules are from the MOs with indices of 70 (~8%) and 67 (~15%), respectively. The 70th MO associated with the TFSA molecule is the fifth highest occupied MO, which corresponds mainly to lone-pairs on the oxygen atoms attached on the electrode surface. The higher occupied MOs contribute less to the conduction band due to the little spatial orbital-band overlap. For the BMIM molecule, on the other hand, the highest occupied MO, which is the π orbital extending over the entire imidazolium ring, contributes to the band the best. Due to the parallel orientation of the imidazolium ring to the electrode surface and the very short distance between the ring and the surface (~3.1 Å), the π orbital greatly overlaps with the unoccupied band of the Au electrode. These results suggest that the electron transfer is easier to occur from the high-lying MOs overlapping with the electrode surface orbitals.

This analysis using MO-projected DOSs was performed also for the interfacial systems displayed in Figure 8 in the main text. We can see from Figure S1b and c the significant decrease in the contribution ratio of the highest occupied MO of the BMIM molecule (i.e.,

the π orbital extending over the imidazolium ring, which is emphasized by the red circle in the figures) to the conduction band near the Fermi level. This indicates, as was expected, that the BMIM molecule releases its electron in the π orbital over the imidazolium ring and the largest contribution depends greatly on the BMIM ring orientation.

Regardless of the BMIM orientation, it is surprising that the low-lying MOs contribute somewhat to the conduction band. This may be due to the large orbital overlap between the electrode and the molecules, which is supported from the fact that the MOs indicating the zero contribution ratio correspond to the fluorine lone-pair orbitals which is clearly distanced from the electrode surface.

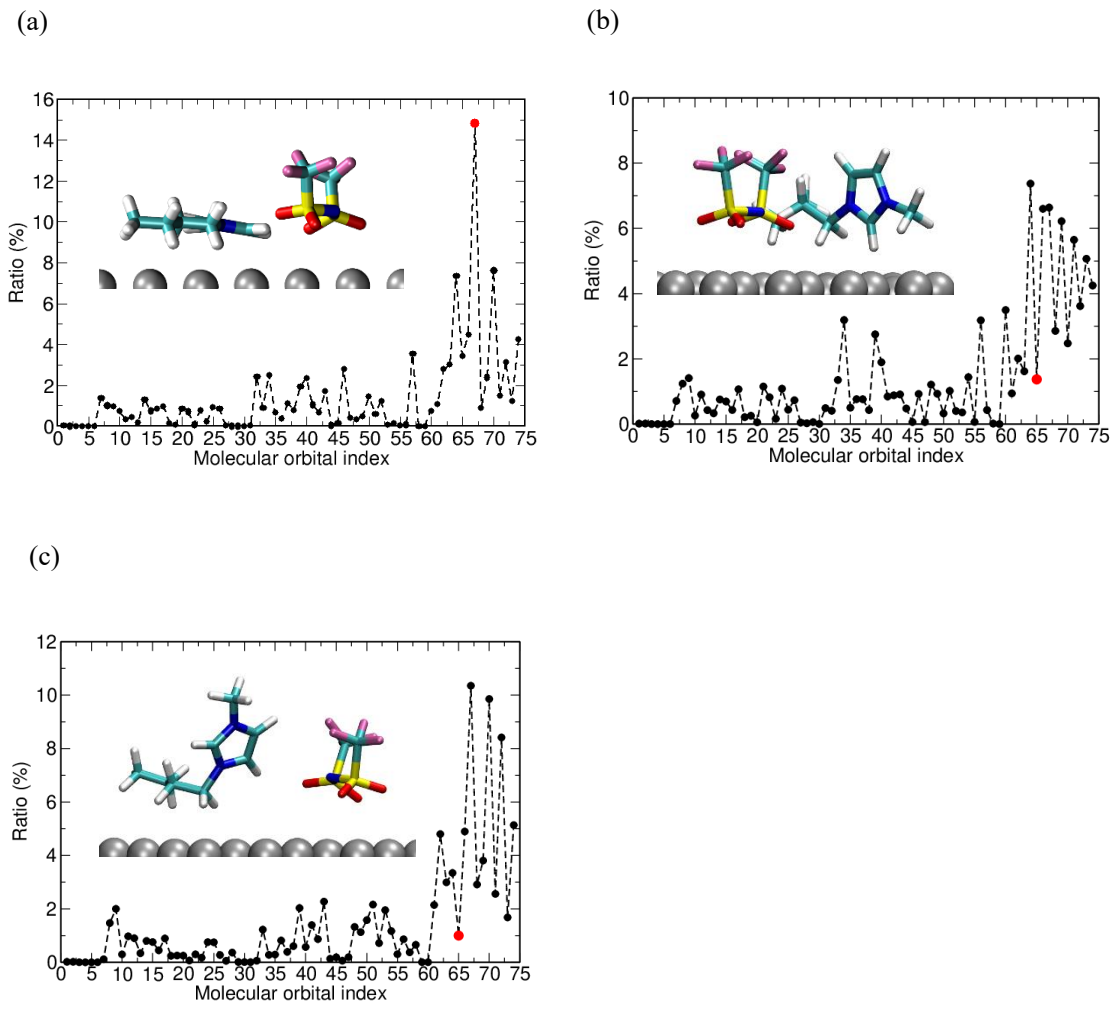

Figure S1. Contribution ratio of each occupied molecular orbital of the isolated IL pair to the conduction band near the Fermi level in the Au/IL system. Note that this is the ratio relative to the total contribution from the IL pair. Panel (a), (b), and (c) correspond to the plots obtained in the systems with the parallel, perpendicular, and tilted orientation of the BMIM molecule, respectively. Red circles indicate the contribution ratio of the highest occupied π molecular orbital in the BMIM molecule. The dashed lines are for the guide of eyes.

4. Adsorption energy of IL molecules on Au electrode surface

The adsorption energies E_{ads}, which are reported in the main text, were calculated using the following expression:

$$E_{ads} = E_{Au/IL} - (E_{Au} + E_{IL}), \quad \text{(S1)}$$

where $E_{Au/IL}$ is the total energy of the Au/IL interfacial system after geometry relaxation, E_{Au} the total energy of the relaxed clean Au electrode surface without the adsorbed IL molecules, and E_{IL} the total energy of the corresponding relaxed free IL molecules. With Grimme's dispersion correction, we obtained E_{ads} of about −7.3 eV as an averaged value (with five different Au/two IL-pairs configurations from each other and its standard error was 0.1 eV). Among the energy, the contribution of dispersion interaction extracted directly from the dispersion correction term was about −8.8 eV. In the present case, the repulsive interaction typified by Pauli exchange reduces the attractive dispersion force by about 1.5 eV. In addition, we obtained E_{ads} by the same calculations as described above except for the absent of Grimme's dispersion correction. The resultant interfacial structure had a large distance between the Au surface and IL molecules by about 0.7 Å compared to the structure obtained from the calculation with the dispersion interaction, leading to E_{ads} of almost zero (0.2 eV with the standard error of 0.1 eV). These calculation data indicate that the dispersion force almost certainly generates the IL adsorption on the Au electrode surface.

5. Supplementary Table

Table S1. Potential changes $\delta\phi_{ele}$ (V) depending on the BMIM orientation [a]

Orientation[b]	Potential change $\delta\phi_{ele}$
parallel	−0.51 (0.01)[c]
perpendicular	−0.37 (0.01)[c]
tilted with distance	−0.15 (0.04)[c]

[a] Potential changes are averaged one obtained from five independent configurations with the respective BMIM orientations.

[b] Imidazolium ring orientation relative to the Au electrode surface. See Figure 5 for the parallel orientation and Figure 8 for the other two orientations.

[c] The value in parenthesis represents standard error.

6. Supplementary Figures

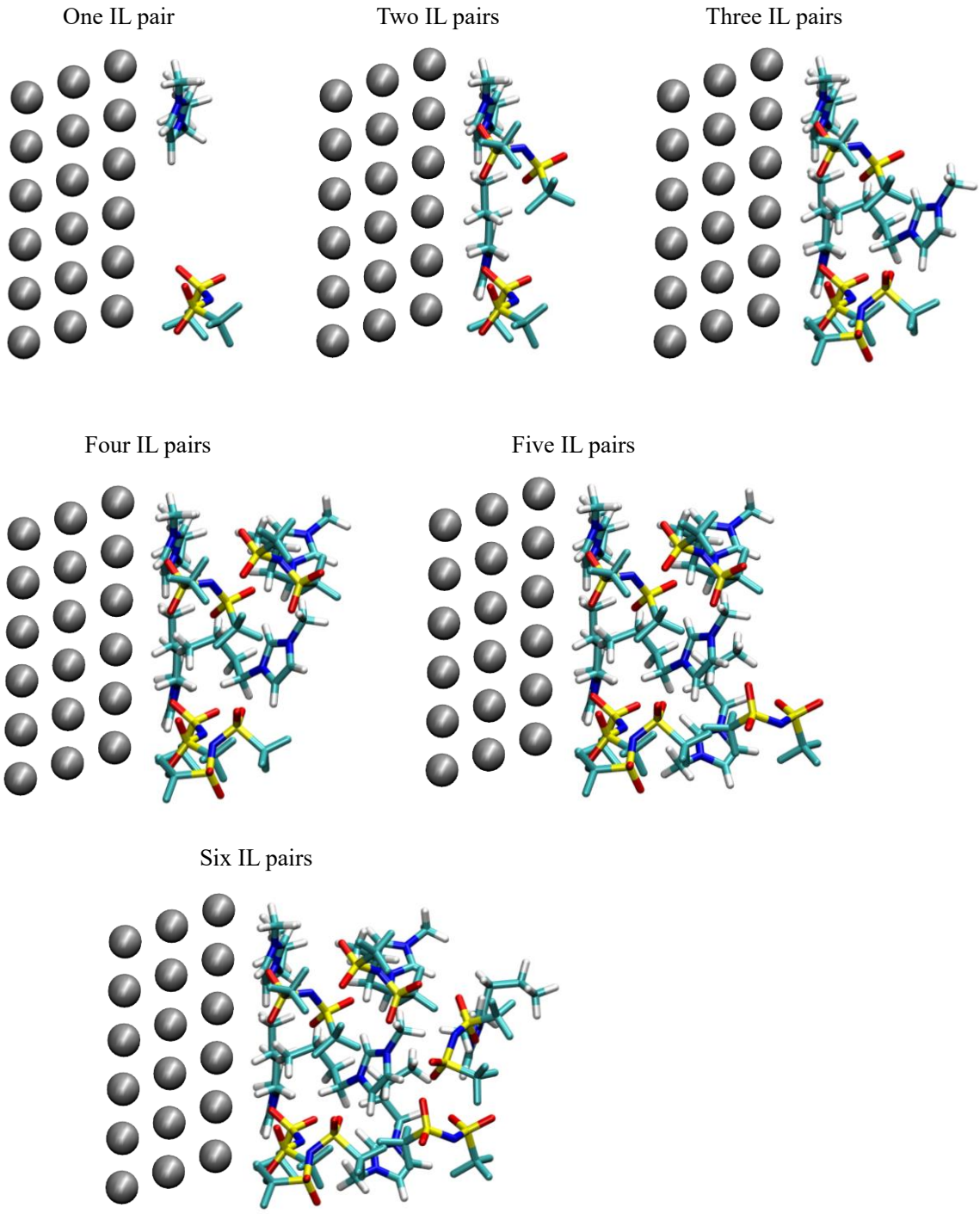

Figure S2. Six Au/IL interfacial systems used to examine the dependence of the number of IL pairs on the potential change of $\delta\phi_{ele}$.

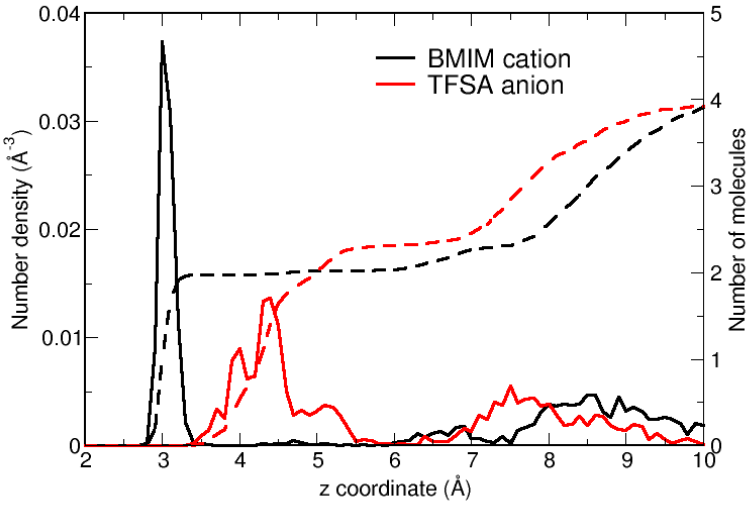

Figure S3. Number density profiles of BMIM (black solid line) and TFSA (red solid line) molecules. Associated integrated number profiles are also plotted by dashed lines (right axis). The electrode surface is placed at the $z = 0$ position. It is found from the plots that there are about two molecules for each ion in the first ionic liquid layer (approximately 2.5-5.5 Å). Note that the profiles are calculated with the center of mass of each ion.

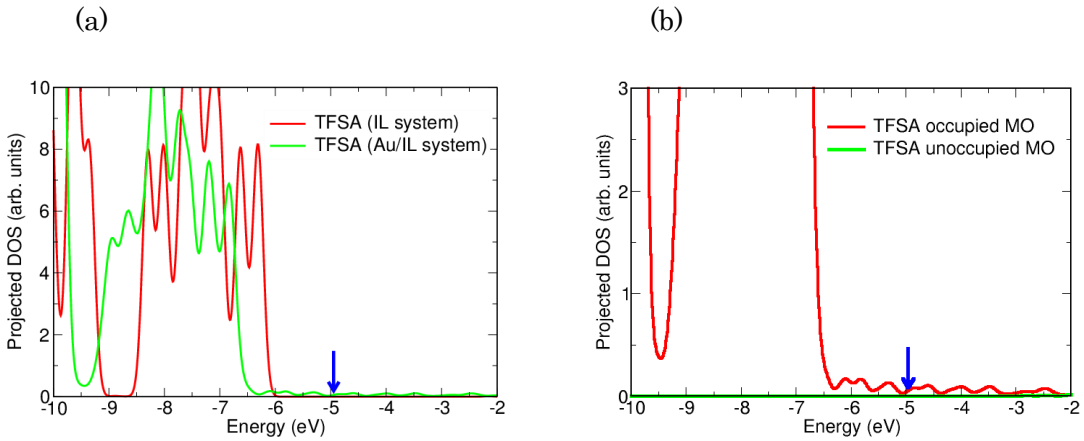

Figure S4. Panel (a): projected densities of states on the TFSA molecule in the isolated IL pair (red line) and the Au/IL system (green line). Panel (b): molecular orbital projected DOSs. Red and green lines represent, respectively, the contributions from the TFSA occupied and unoccupied molecular orbitals (MOs). Note that the green line in the panel (b) identical almost to the horizontal axis line. Blue arrows indicate the Fermi level in the Au/IL system. Energy zero is set to the vacuum level outside the IL molecules.

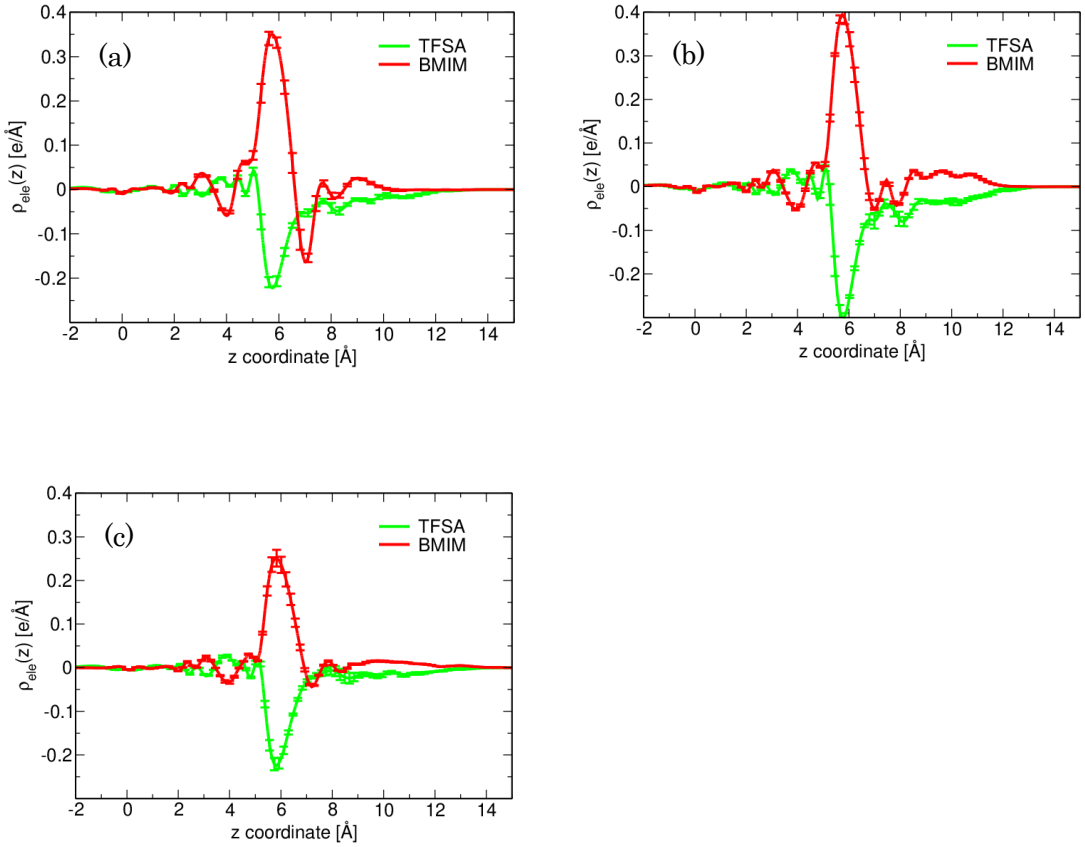

Figure S5. Electron density change profiles for the systems with an imidazolium-ring orientation parallel to the electrode surface (panel a), with a perpendicular orientation to the electrode surface (panel b), and with a tilted imidazolium-ring orientation with a distance from the electrode surface (panel c). See Figure 8 in the main text for the latter two orientations of the BMIM molecule. These profiles are averaged ones using five interfacial systems with different TFSA configurations, for the respective Figure 6, Figure 8c, and 8d in the main text. Standard errors are displayed in the figures, which are not more than 0.02 e/Å. This indicates that the electron redistribution associated with the BMIM molecule is almost independent on the TFSA configurations.

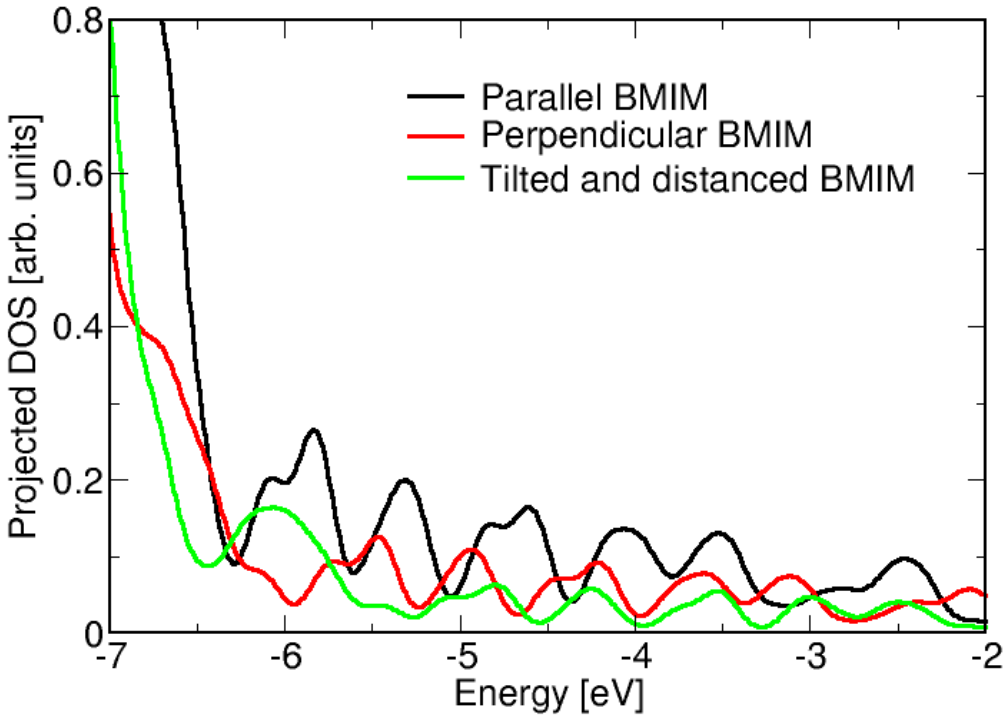

Figure S6. Projected DOSs onto the occupied molecular orbitals (MOs) of the BMIM molecule in the isolated IL system. Black, red and green lines correspond, respectively, to the plots obtained in the Au/IL system with the parallel, perpendicular, and tilted orientation of the BMIM molecule. The Fermi energies in the systems are −4.95, −4.58, and −3.85 eV, respectively. Qualitative decrease in the MO-projected DOS can be observed in the order of black, red, and green plots.

References

S1. H. Andersen, *J. Comput. Phys.*, 1983, **52**, 24-34.

S2. R. W. Hockney, J. W. Eastwood, *Computer Simulation Using Particles*, Taylor & Francis Group, 1988.

S3. S. K. Reed, O. J. Lanning, P. A. Madden, *J. Chem. Phys.*, 2007, **126**, 084704.

S4. T. Köddermann, D. Paschek, R. Ludwig, *Chem. Phys. Chem.*, 2007, **8**, 2464–2470.

S5. H. Heinz, R. A. Vaia, B. L. Farmer, R. R. Naik, *J. Phys. Chem. C*, 2008, **112**, 17281–17290.

S6. E. S. C. Ferreira, C. M. Pereira, M. N. D. S. Cordeiro, D. J. V. A. dos Santos, *J. Phys. Chem. B*, 2015, **119**, 9883–9892.